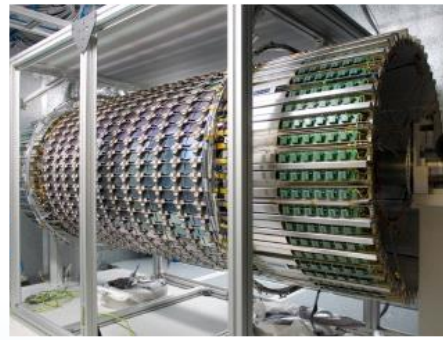
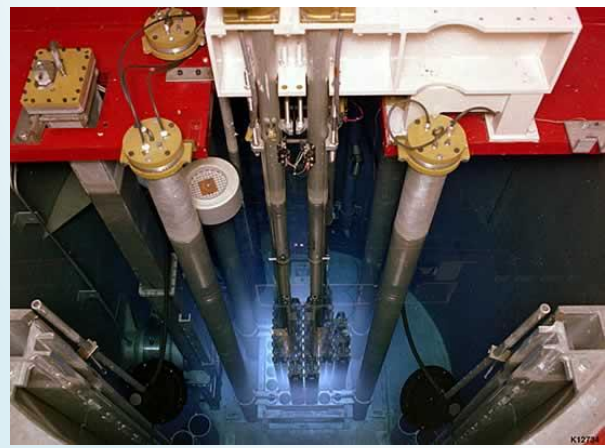
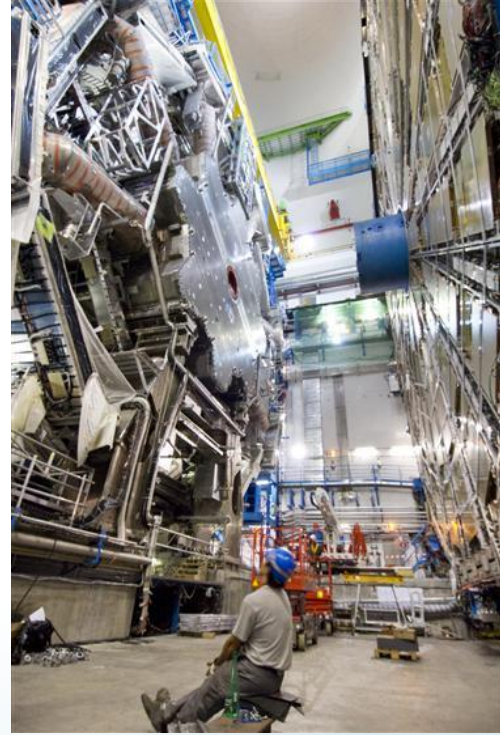
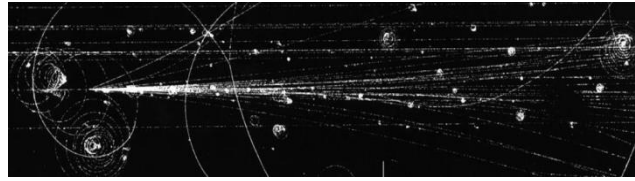
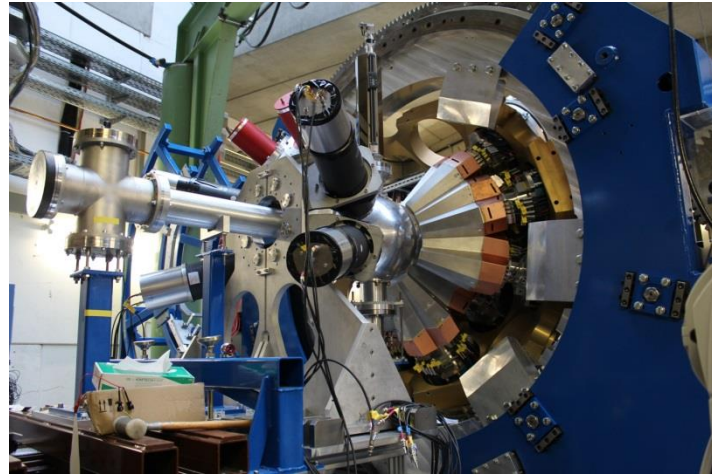


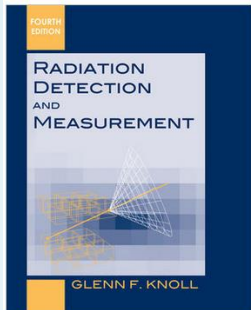
# Interactions of Particles with Matter-II

Phil Allport ([allport@cern.ch](mailto:allport@cern.ch)) University of Birmingham



# General Approach Used in these Lectures

- These lectures will concentrate on physics rather than formulae and assume students seeking formulae will refer to the appropriate literature and primary sources, many of which can be found in the reviews at <https://pdg.lbl.gov/>



Another excellent resource is **Radiation Detection and Measurement** by **Glenn Knoll** (ISBN: 978-0-470-13148-0)

- A fairly recent review of [silicon detectors](#) may be of interest as it contains a number of useful references and links to [supplementary information](#)
- Further recommended books include: **Evolution of Silicon Sensor Technology in Particle Physics** by F. Hartmann (ISBN: 978-3-319-64436-3) and **Particle Detectors: Fundamentals and Applications** by H. Kolanoski and N. Wermes (ISBN-13: 9780198858362)

PDG particle data group

NEWS: Help PDG determine which products to keep in the future. Please answer our survey.

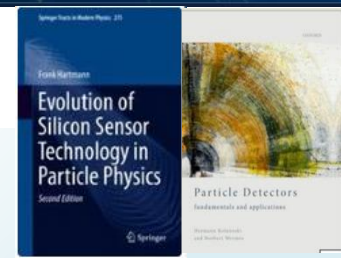
## Reviews, Tables & Plots

P.A. Zyla *et al.* (Particle Data Group), *Prog. Theor. Exp. Phys.* 2020, 083C01 (2020) and 2021 update.  
Files can be downloaded directly by clicking on the icon:

[Expand/Collapse All](#)

- Introduction, History plots, Online information
- Constants, Units, Atomic and Nuclear Properties
- Standard Model and Related Topics
- Astrophysics and Cosmology
- Experimental Methods and Colliders

Accelerator physics of colliders (rev.)	
High-energy collider parameters	
Neutrino beam lines at High-energy proton synchrotrons (rev.)	
Passage of particles through matter (rev.)	
Particle detectors at accelerators (rev.)	
Particle detectors for non-accelerator physics (rev.)	
Radioactivity and radiation protection (rev.)	
Commonly used radioactive sources (rev.)	



# Overview of Topics to be Covered

## Lecture I

- Natural sources of radiation and their detection
  - Important in its own right and essential for understanding tools for testing detectors
- Ionising radiation
  - Charged particle interactions (ions and electrons)
  - Neutral particle detection (indirect detection)
- Non-ionising interactions with matter
  - Lower energy phenomena
  - Higher energy interactions
  - Factors affecting EM and hadron calorimetry

## Lecture II

- Efficiencies and energy resolutions for individual sensors
- Brief overview of silicon sensor technologies
  - Overview of different types of sensors
  - Recap of operating principles
- Digressing into gaseous tracking detectors
  - Signal formation in sensors without and with gain
- Application for signal formation in simple diode (two terminal) case

# Sensor Efficiency (some definitions):

Efficiency measures the probability of detecting radiation:

The intrinsic efficiency of a detector for a given type of radiation is defined by

$$\varepsilon_{int} = \frac{\text{no. of pulses detected}}{\text{no. of radiation quanta incident on the detector}}$$

For charged particles,  $\varepsilon_{int} \approx 1$  but for neutrons or gammas  $\varepsilon_{int} \ll 1$

The absolute efficiency for a given measurement is defined by

$$\varepsilon_{abs} = \frac{\text{no. of pulses detected}}{\text{no. of radiation quanta emitted by the source}}$$

Absolute efficiency depends on geometry as well as the intrinsic efficiency.

For a point source emitting uniformly in all directions ,

$$\varepsilon_{abs} = \frac{\Omega}{4\pi} \varepsilon_{int}$$
 where  $\Omega$  is the solid angle subtended by the detector.

# Intrinsic Sensor Energy Resolution:

Some detectors produce a pulse whose size is ideally proportional to the energy deposited.

But random fluctuations mean there is always some spread in pulse sizes even when exactly the same energy **E** is deposited.

Suppose the pulse consists of (on average)  $\bar{N}$  signal carriers.

$\bar{N} = \frac{E}{w}$  where **w** is the energy required (on average) to create a signal carrier.

If these signal carriers can be considered independent, the random process by which they are created obeys Poisson statistics:

the number **N** fluctuates with variance equal to the mean ( $\bar{N}$ ), so with a **standard deviation** equal to  $\sqrt{\bar{N}}$ .

# Intrinsic Sensor Energy Resolution:

Poisson statistics describe independent random events (like radioactive decay).

However, when a particle deposits its energy there is a fixed amount of energy, there are different ways the energy can be absorbed and the possible detector responses are quantised.

This means the ionisation events are not truly independent, and this constraint reduces the fluctuations possible (improving the resolution).

Incorporate this by introducing a multiplicative factor  $F$ , the “**Fano factor**”, so that the variance is equal to  $F\bar{N}$ .

$$F \leq 1, \quad (F \approx 1 \text{ if only a small part of the energy gives signal carriers})$$

The **standard deviation** is then  $\sqrt{F\bar{N}}$

# FANO Factor:

## Theoretical values

(For some more justification of this see reference page 29 at [http://www-physics.lbl.gov/~spieler/Heidelberg\\_Notes\\_2005/pdf/II\\_Signal\\_Formation.pdf](http://www-physics.lbl.gov/~spieler/Heidelberg_Notes_2005/pdf/II_Signal_Formation.pdf) from the very useful notes at <http://www-physics.lbl.gov/~spieler/>)

Si:	0.115
Ge:	0.13
GaAs:	0.12
Diamond:	0.08

## FANO Factor: Some measured values

Ar (gas):	$0.20 \pm 0.01/0.02$
Xe (gas):	0.13 to 0.29
CZT:	$0.089 \pm 0.005$

# Intrinsic Sensor Energy Resolution:

For large  $\bar{N}$ , the Poisson distribution is approximated by the Gaussian distribution (mean  $\bar{N}$ , standard deviation  $\sigma$ ):

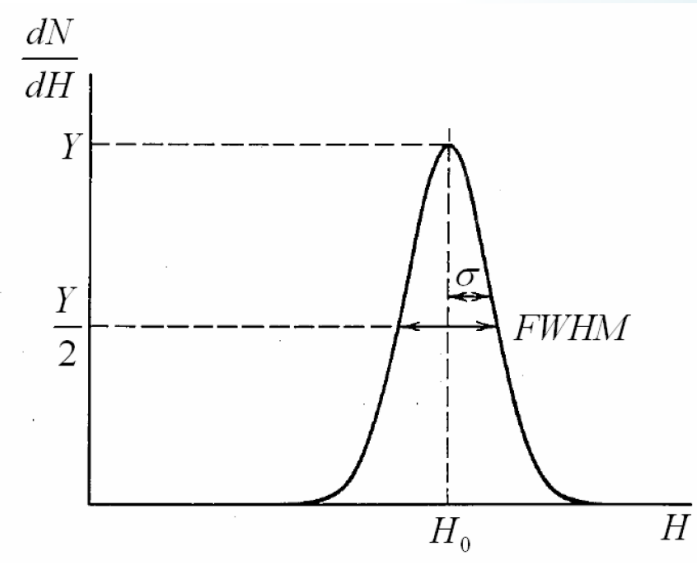
$$P(N) = \frac{1}{\sqrt{2\pi}\sigma} \exp\left(-\frac{(N-\bar{N})^2}{2\sigma^2}\right)$$

Experimentally, have a spectrum of pulse heights  $H$ , and often measure the full-width at half-maximum (FWHM).

For a Gaussian distribution this is equal to

$$2\sqrt{2\ln 2}\sigma = 2.35\sigma$$

where  $\sigma$  is the **standard deviation** of this distribution.



# Intrinsic Sensor Energy Resolution:

The **energy resolution** of the detector is conventionally defined as  $\frac{\text{FWHM}}{H_0}$

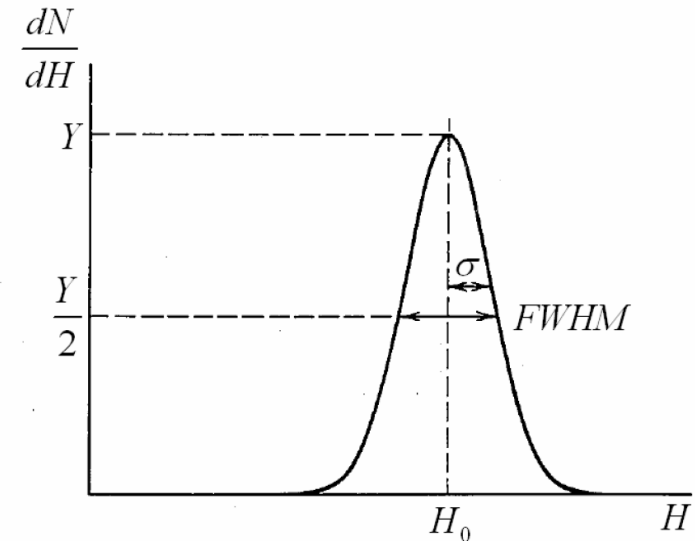
(can distinguish two peaks if they are separated by more than the FWHM).

Assuming that the experimental pulse height (measured for example in volts) is directly proportional to the number of signal carriers,

$$H = KN ; H_0 = K\bar{N}$$

then the FWHM of the pulse height spectrum is equal to  $2.35\sigma = 2.35K\sqrt{F\bar{N}}$

and the **energy resolution** is equal to  $\frac{2.35K\sqrt{F\bar{N}}}{K\bar{N}} = 2.35\sqrt{\frac{F}{\bar{N}}} = \boxed{2.35\sqrt{\frac{Fw}{E}}}$



# Position-sensitive Semiconductor Detectors <sup>10</sup>

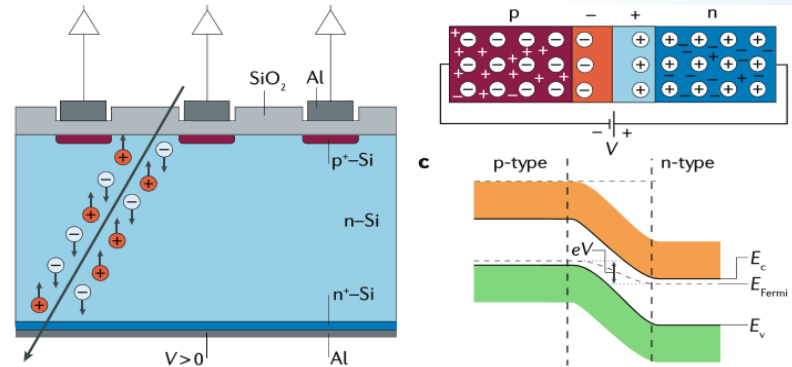
For tracking need to obtain precise positional information.

**Semiconductors can be used to do this in a large number of ways:**

- (Resistive charge division\*)

\*Radeka & Rehak BNL-25070 CONF-781033-8

- Strip detectors
- Silicon drift detectors
- Hybrid pixel detectors
- Charge coupled devices
- Monolithic pixel detectors
- Timing (4D)\*
- 3D Pixels\*



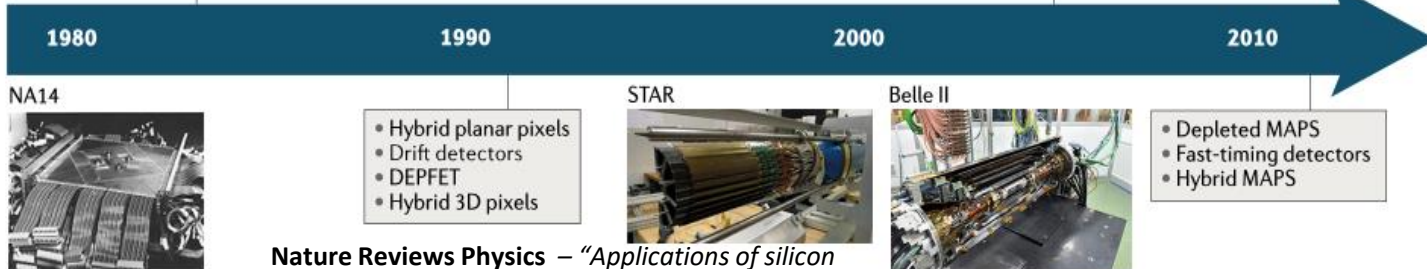
- Silicon strips
- Multiplexing ASICs
- CCDs



- CMOS MAPS
- Silicon-on-insulator pixels
- Vertical 3D integration



\*Francisca Munoz Sanchez (10/5/22)



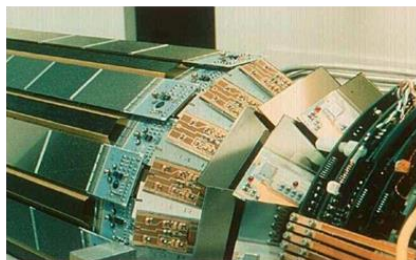
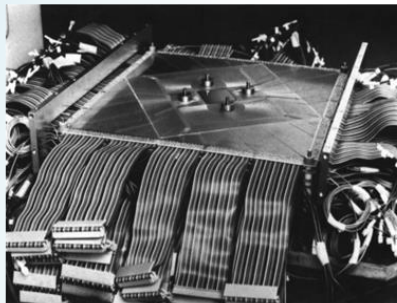
Nature Reviews Physics – “Applications of silicon strip and pixel-based particle tracking detectors” - <https://doi.org/10.1038/s42254-019-0081-z>

**Most of the sensor technologies discussed here will be based on segmented planar reverse-biased p-n junction diodes.**

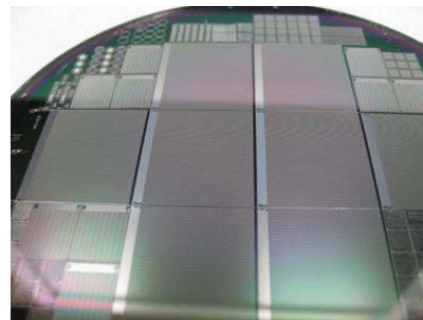
# Silicon Strip Detectors

Historical development over 4 decades.

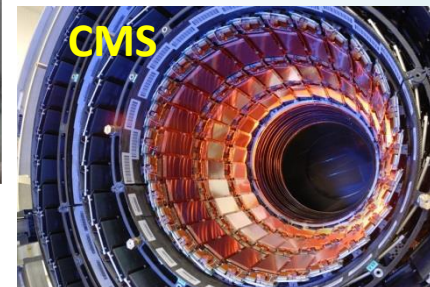
Na14 silicon vertex detector



ALEPH detector  
DELPHI detector



ATLAS detector  
CMS detector

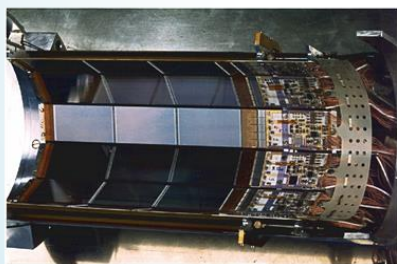


1980s

1990s

2000s

2010s



Opal silicon microvertex detector

H1 detector  
ZEUS detector  
CDF  
DO



# Fast Recap of p-n Junction

A p-n junction\* consists of a single crystal of semiconductor, one surface of which is doped p-type and the other end n-type.

At the junction, electrons diffuse from the **n-type** material, leaving behind **fixed +ve charges** on the donor atoms.

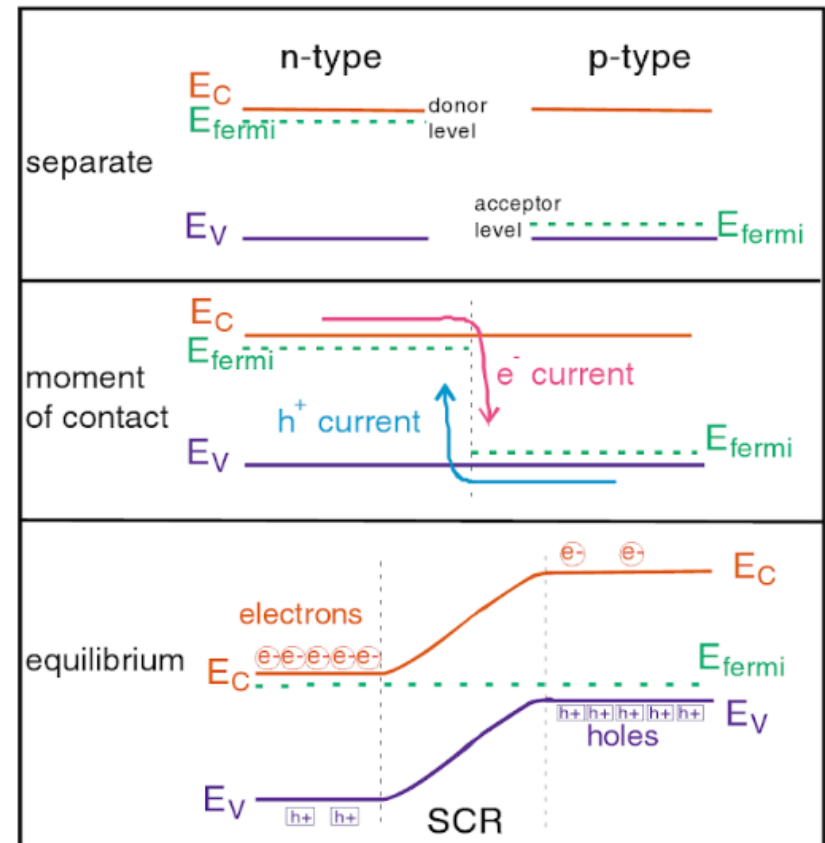
Similarly, holes diffusing from the **p-type** into the n-type, leave **fixed -ve charges** on the acceptor atoms.

Diffusion continues until the electric field due to the fixed charges becomes so large that it prevents further diffusion.

This creates a “depletion layer” (**S**pace **C**harge **R**egion) with effectively no majority charge carriers.

Gives **-ve potential** on **p-type side** (repels electrons).

\*Francisca Munoz  
Sanchez (10/5/22)



Space Charge Region formed at interface which because of diffusion across the boundary is depleted of free carriers.

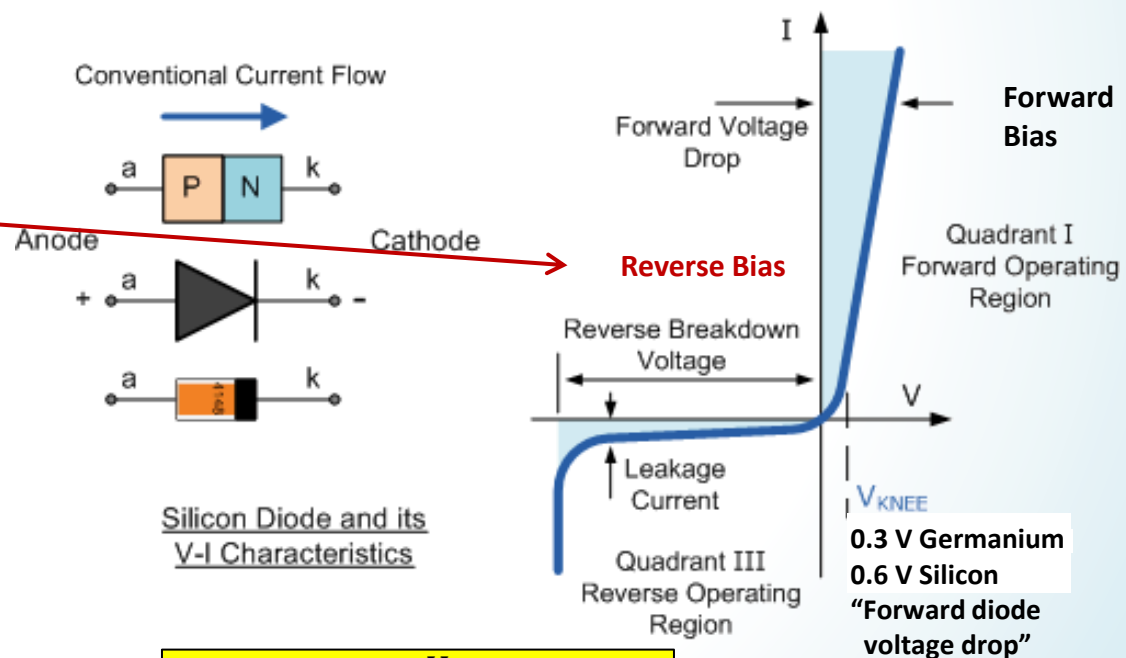
# Fast Recap of p-n Junction

Junction acts as a diode.

If one applies a +ve voltage to the p-type side, electrons from the n-type side will be attracted and a large current will flow across the junction, but if one applies a -ve voltage to the p-type side the only current is due to the minority carriers.

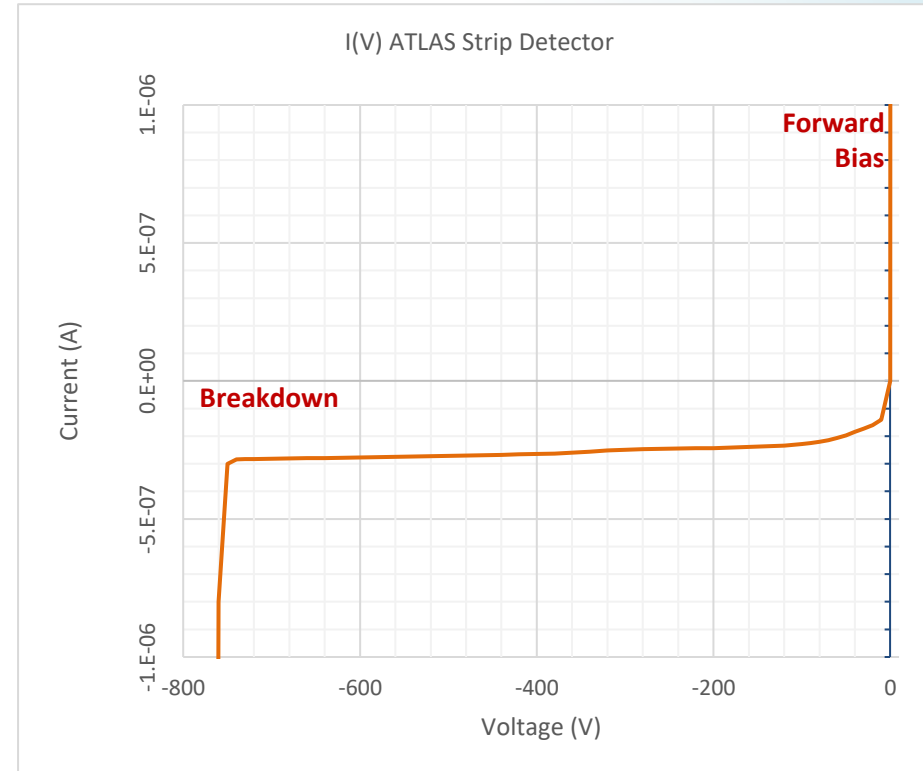
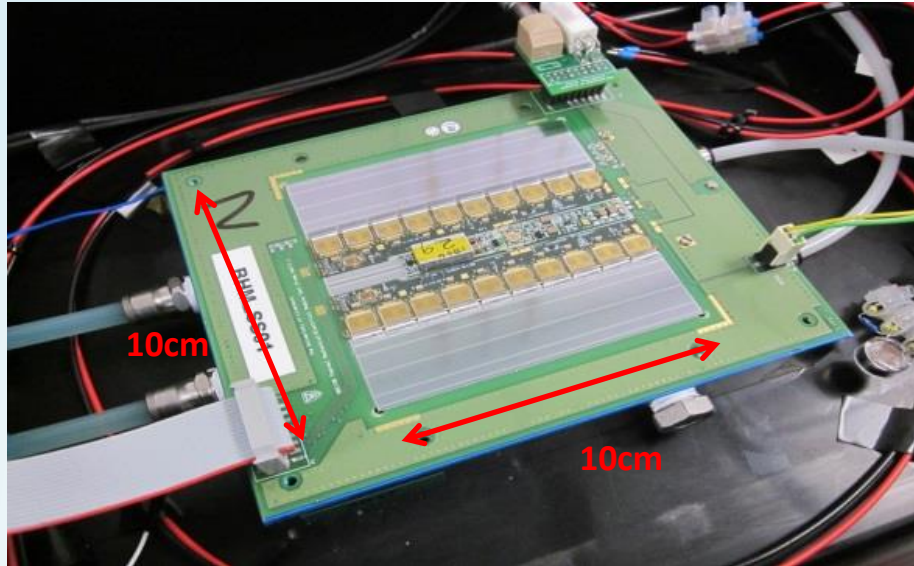
To make a useful detector, the p-n junction is operated in this “**reverse bias**” mode.

**A voltage is applied which pushes the electrons and holes further apart, increasing the thickness of the depletion layer and generating a large electric field across it.**

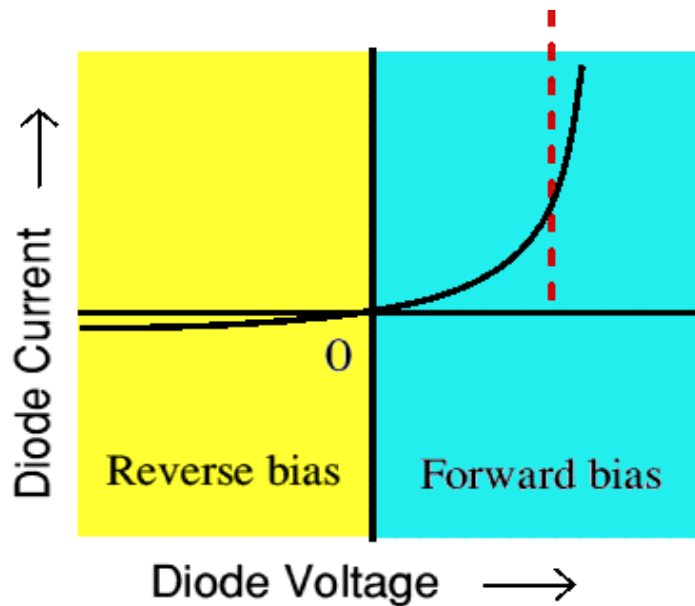


$$J = J_0 (e^{qV/kT} - 1)$$

# Fast Recap of p-n Junction



Diode Voltage Drop



$$J = J_n + J_p \text{ (current density)}$$

$$= J_0 \left( e^{qV/kT} - 1 \right)$$

# Space Charge Region (SCR)

Poisson's equation  $\nabla^2 \varphi = -\frac{\rho}{\epsilon}$  relates potential  $\varphi$  to charge density  $\rho$  ( $\epsilon$  is the dielectric constant of the material). In 1D have  $\frac{d^2 \varphi}{dx^2} = -\frac{\rho}{\epsilon}$

Within the depletion layer, assume **all dopants ionised**,

→ charge density  $eN_D$  on **n-type** side &  $-eN_A$  on **p-type** side

Suppose SCR extends distance **a** into **n-type** and **b** into **p-type**

Integrating once, gives the electric field  $E = -\frac{d\varphi}{dx}$  as linear

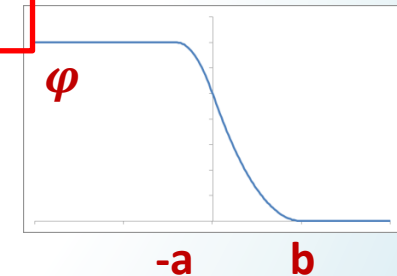
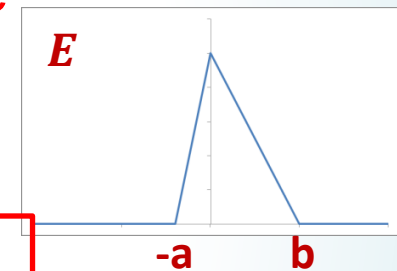
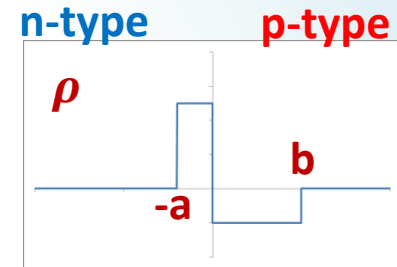
The solution with  $E = 0$  outside the depletion layer is

$$E = \frac{eN_D}{\epsilon}(a+x) \text{ for } -a < x < 0, \quad E = \frac{eN_A}{\epsilon}(b-x) \text{ for } 0 < x < b$$

Since  $E$  must be **continuous** at  $x = 0$  we require  $aN_D = bN_A$  (conserves charge): **SCR** deeper on side with lower doping.

Integrating again,  $\varphi = -\frac{eN_D}{2\epsilon}(x+a)^2 + V$  for  $-a < x < 0$

$$\varphi = +\frac{eN_A}{2\epsilon}(x-b)^2 \text{ for } 0 < x < b \text{ (choose potential zero at } x = b).$$



# Depletion Depth (SCR Width)

Since the potential must be **continuous** at  $x = 0$ , require  $\frac{eN_A b^2}{2\epsilon} = V - \frac{eN_D a^2}{2\epsilon}$

This is the relationship between applied voltage and depletion layer (SCR) thickness

$$V = \frac{eN_A b^2}{2\epsilon} + \frac{eN_D a^2}{2\epsilon} = \frac{e}{2\epsilon} N_A (a + b)b = \frac{e}{2\epsilon} N_D (a + b)a$$

Suppose (as drawn opposite)  $N_D \gg N_A$  so that  $b \gg a$   
( $aN_D = bN_A$ ),

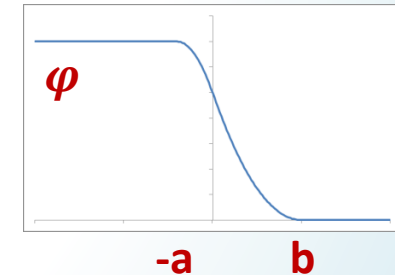
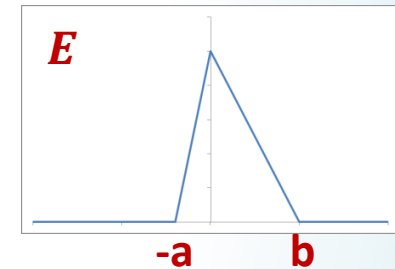
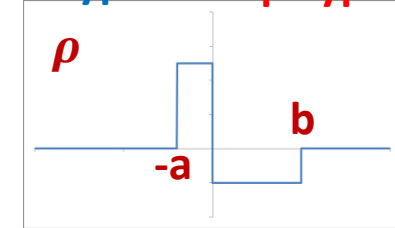
then  $a + b \approx b$  so  $V \approx \frac{eN_A}{2\epsilon} b^2$  or  $b \approx \sqrt{\frac{2\epsilon V}{eN_A}}$

(if instead  $N_A \gg N_D$  would derive  $a \approx \sqrt{\frac{2\epsilon V}{eN_D}}$ )

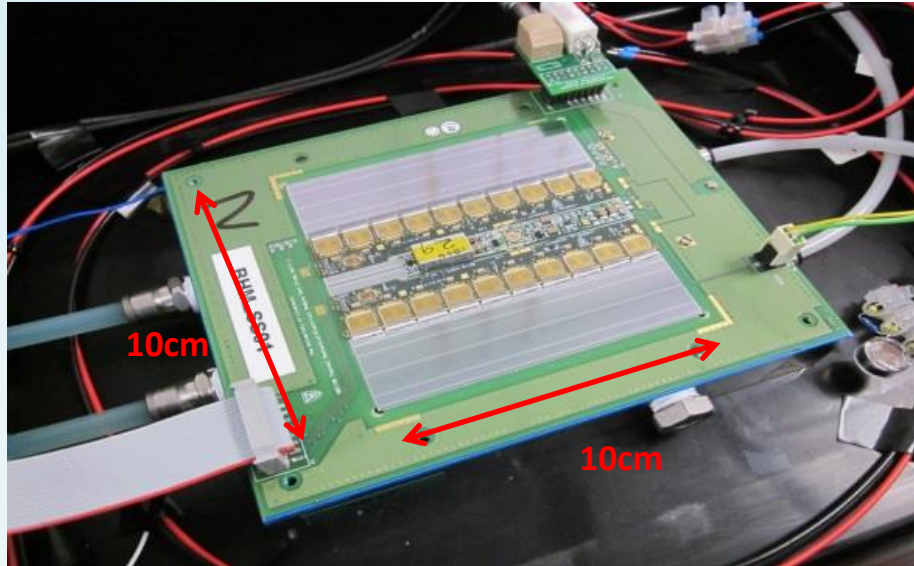
The thickness of the depletion layer is proportional to  $\sqrt{\frac{V}{N_{min}}}$

where  $N_{min}$  is the lower of the two dopant concentrations.

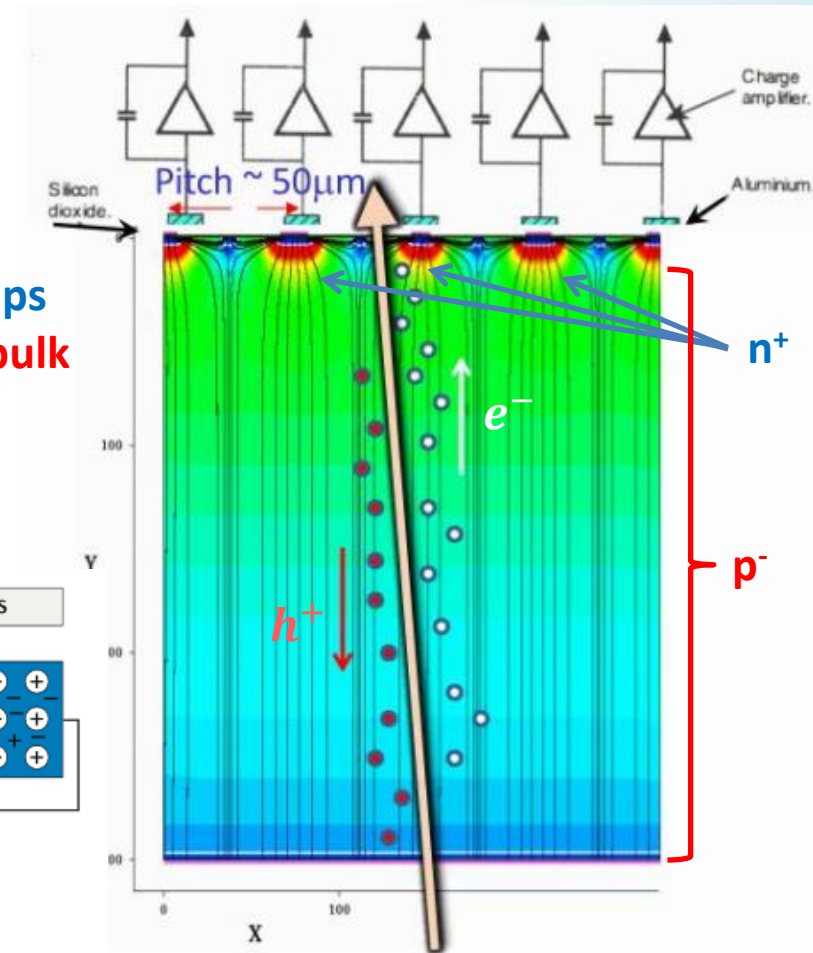
n-type p-type



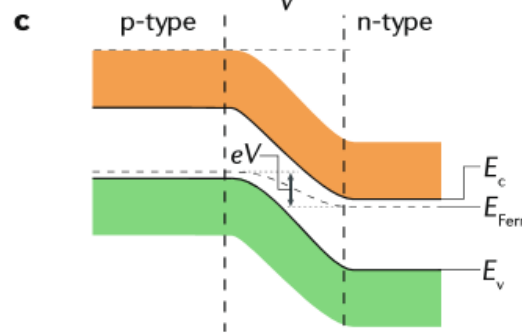
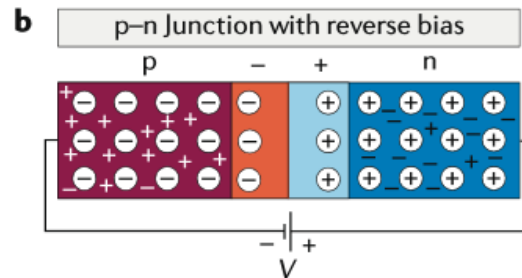
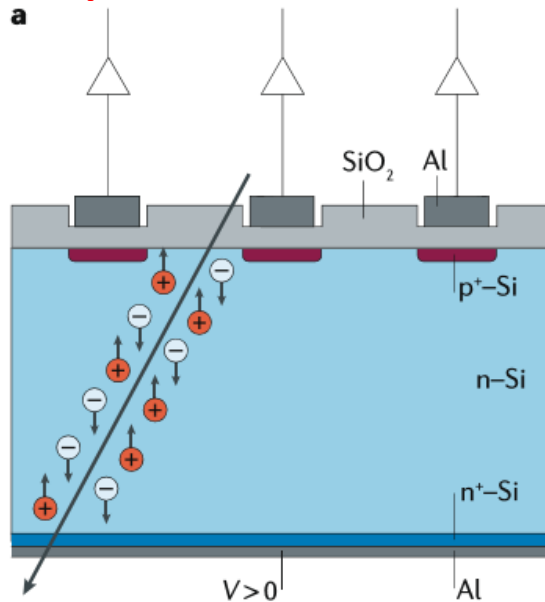
# Depletion Layer (Space Charge Region)



$n^+$  strips in  $p^-$  bulk

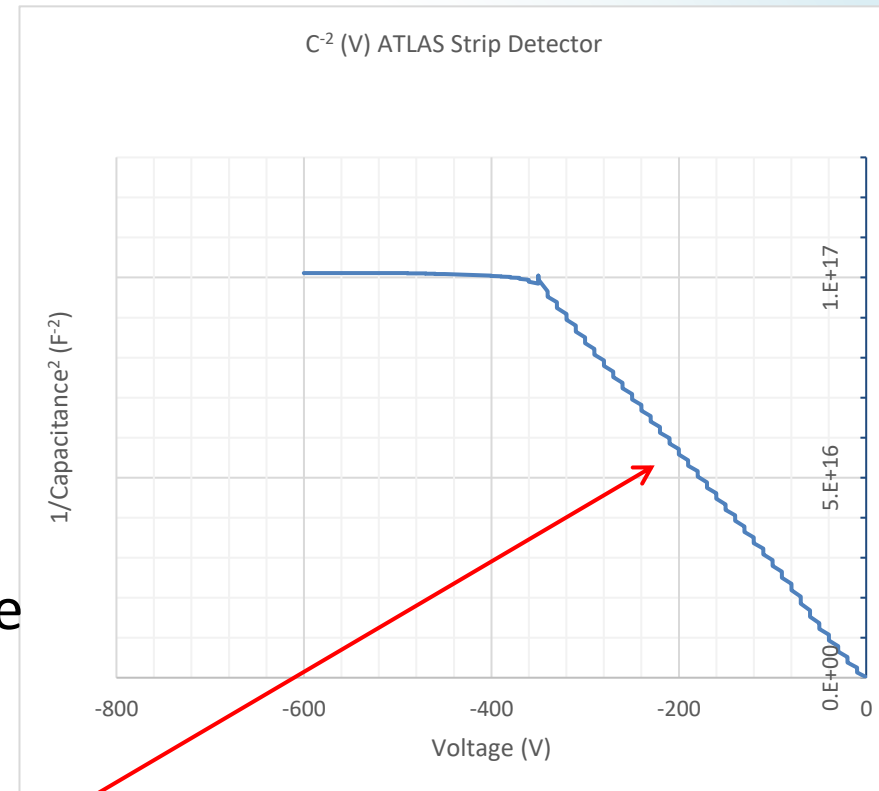
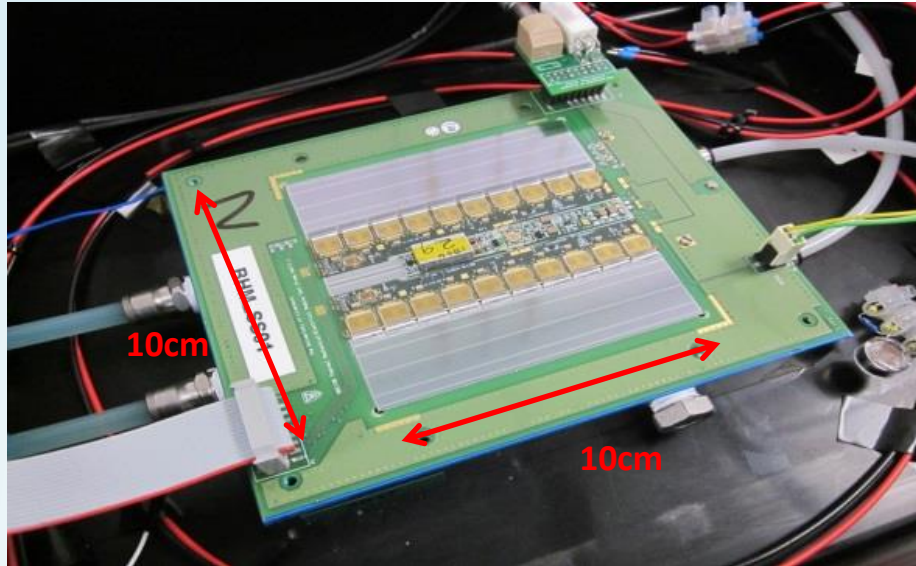


$p^+$  strips in  $n^-$  bulk



On average about **3.6eV** of deposited energy required for each  $eh$ -pair produced.

# Depletion Layer (Space Charge Region)



$C(V) = \frac{\epsilon_0 \epsilon_r \rho_{Si} A}{d(V)}$  giving capacitance per unit area,  $A$ , varying as  $1/C^2 \propto V$ .

The slope of the linear part of  $C^{-2}(V)$  can then be used to derive  $N_{min}$  and hence substrate resistivity  $\left( = 1/q\mu_{h,e}N_{min} \right)$  with mobility,  $\mu_{h,e}$ ,

given, for  $V \gg V_{bi}$ , that

$$\frac{\partial(1/C^2)}{\partial V} = \frac{2}{qN_{min}\epsilon_0\epsilon_r\rho_{Si}}$$

# Silicon Strip (1D) Detectors

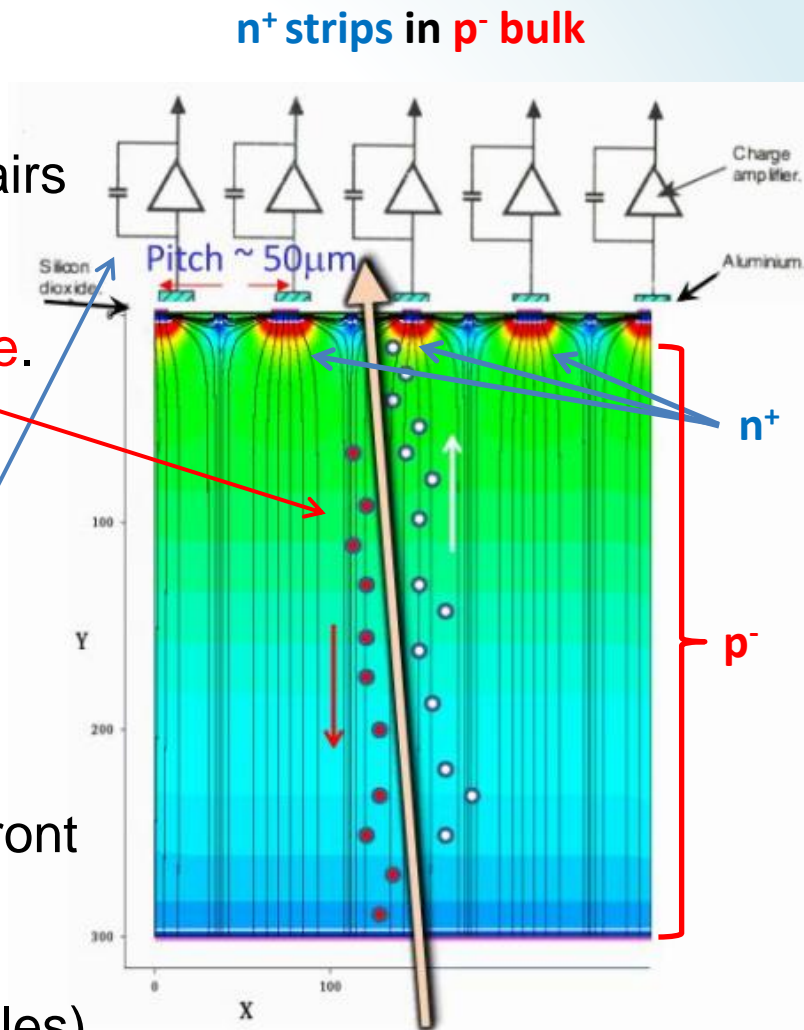
When a fast charged particle travels through the depletion layer it creates electron-hole pairs along its track.

Due to the electric field, the **charges separate**.

Detect a pulse corresponding to the voltage drop across the detector as the charges separate (for example measured across a resistor in series with the detector or by a **current integrator amplifier circuit**).

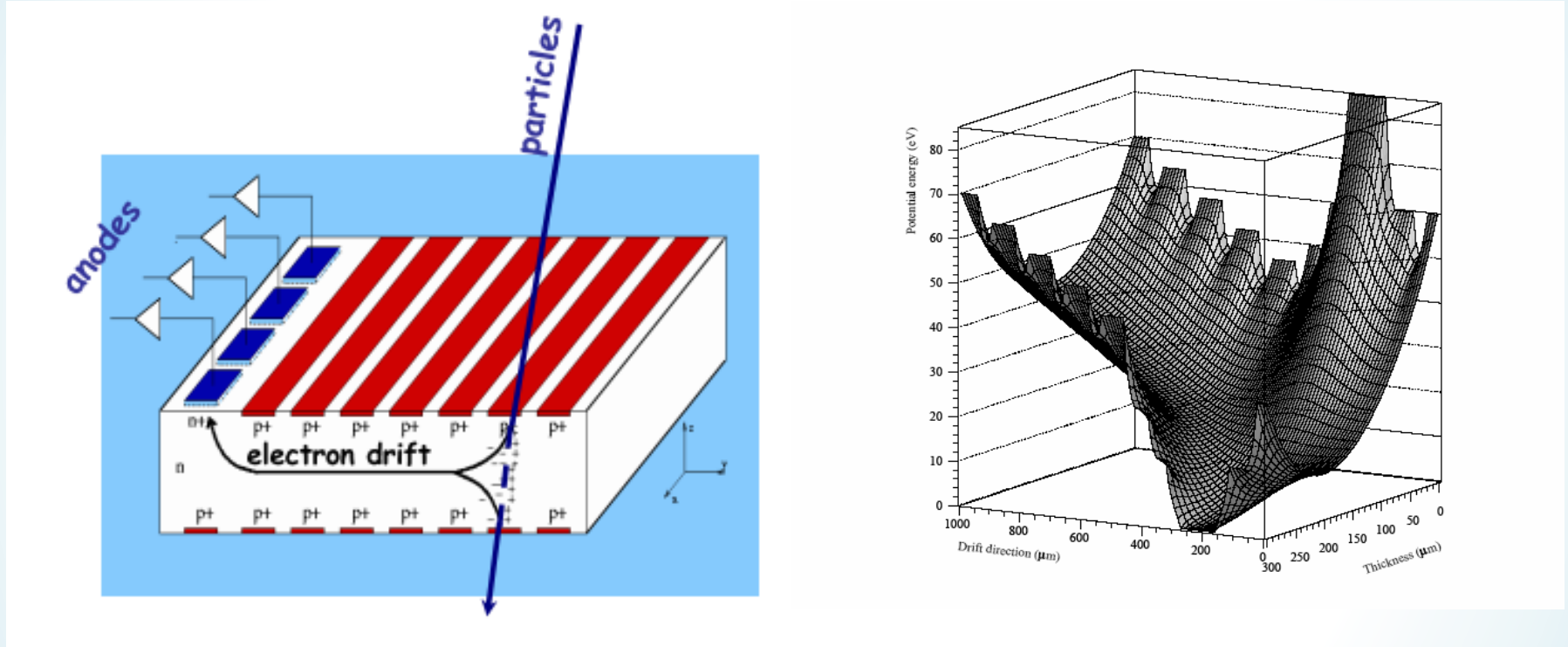
Detector is connected using metallic layers front and back (often aluminium).

For detecting charged ions (e.g. alpha particles) one needs the metal layer at the surface facing the incident particles to be as thin as possible and the depletion layer to extend as close to it as possible.



# Silicon Drift Detectors

Signal is drifted in the silicon (like a gas drift detector) so the second readout coordinate is determined from the drift time.



Suffer from material inhomogeneities (mobility,  $\mu$ , variation with position) and poor radiation tolerance.

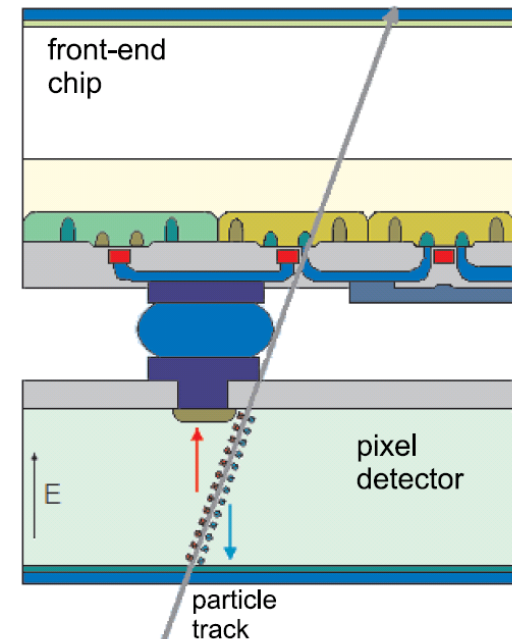
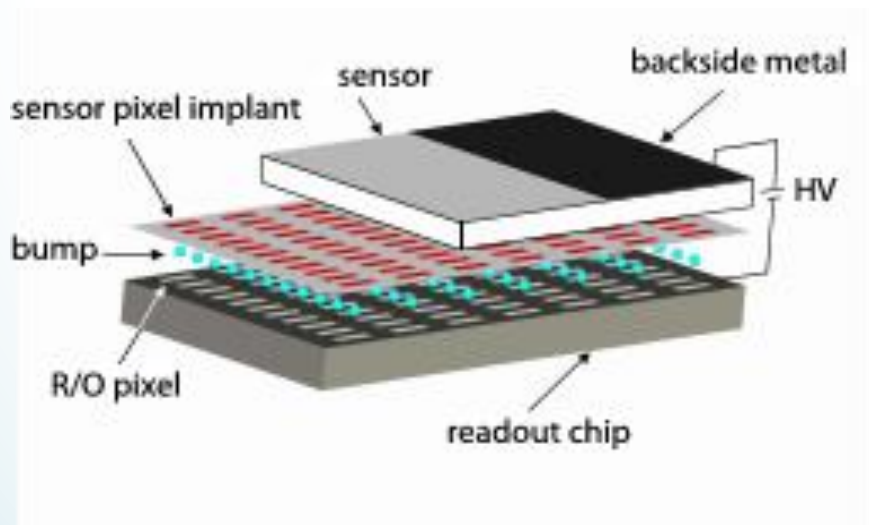
$$( \underline{v}_{\text{Drift}} = \mu \underline{E} )$$

# Pixel Detectors

Instead of dividing the contacts into strips, could divide it into a 2D array of small metallic contacts, separated by insulating  $\text{SiO}_2$ , to give individual pixels.

Problem is that one then needs to take a separate output from each pixel. Can connect a second silicon microelectronics wafer via bump bonding.

The use of such sensors is increasing. For the future look also to monolithic pixel chips (discussed below).



# Charge Coupled Device (CCD)

Consists of a p-n junction with an insulating ( $\text{SiO}_2$ ) layer just below the +ve contact. When radiation releases electrons and holes, electrons drift towards the +ve contact but then trapped behind the insulating layer.

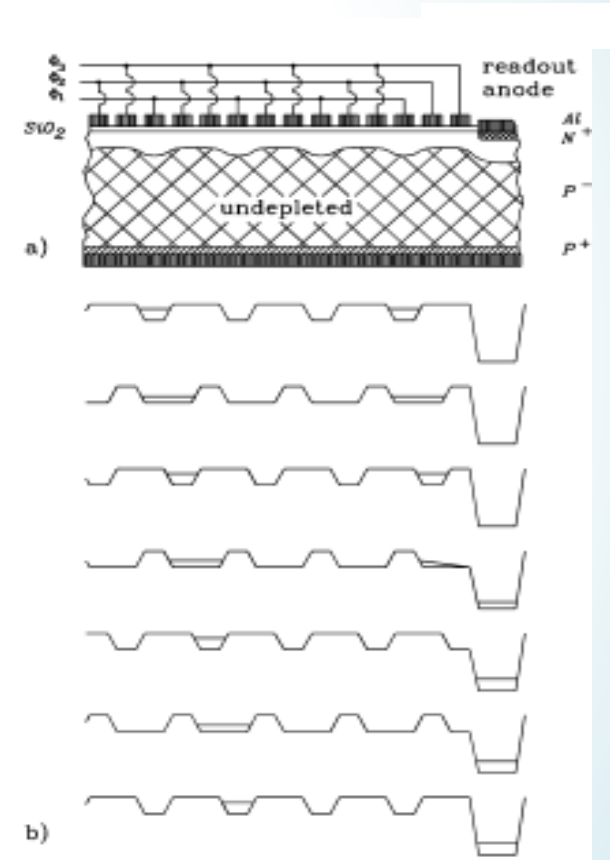
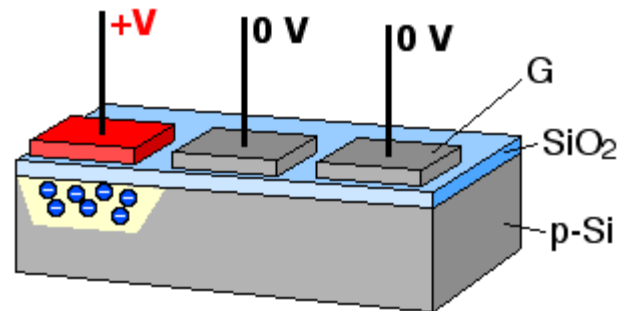
+ve contact is divided into an array of small pads.

Free electrons collect behind the nearest +ve pad.

When it is time to read out the charge, voltage is stepped across the pads, pulling the electrons.

When the electrons reach the edge of the device they can be collected or clocked in the orthogonal direction to give a single readout.

Determine the charge collected behind each pixel.



However, readout is slow (as highly serial) and even lowish levels of radiation can impact the **charge transfer efficiency** → poor radiation tolerance.

# Charge Coupled Device (CCD)

Generally need to mask the detector during readout to avoid signal smearing across pixels.

CCDs are widely used for optical imaging in astronomy as pixel response is very uniform. When CCDs are used in digital cameras, generally use an “interline” architecture, where alternate columns are permanently masked. After exposure the image is rapidly shifted by one column, and then these columns are read out without any problem of smearing.

Pixel sizes can be  $\lesssim$  few  $\mu\text{m}$ .

CCDs can also be used for X-ray imaging, or detecting particles\*.

Outside niche scientific instruments, most commercial systems moving to CMOS Imaging Sensors.

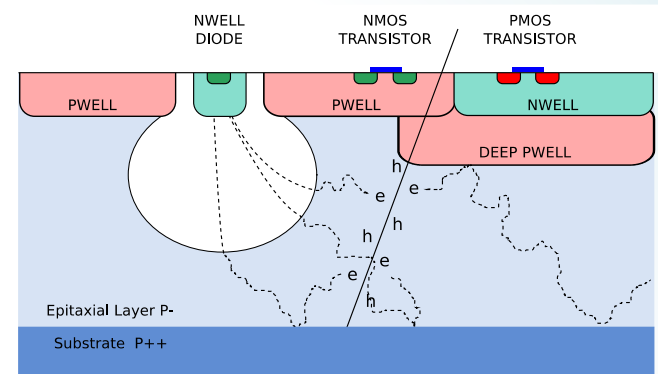
\*Daniel Weatherill (31/5/22)

# Monolithic Pixel Detectors

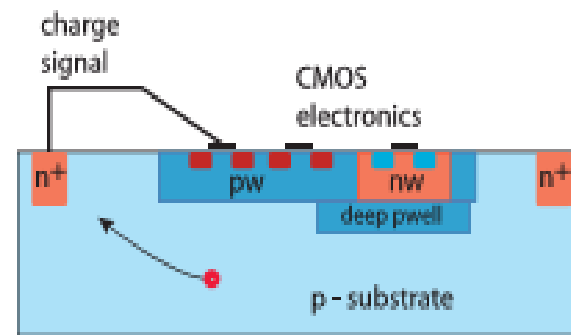
Can combine the read-out microelectronics (silicon) with the sensor (silicon) into a single (monolithic) detector\*.

Readout is CMOS and technologies for combined CMOS Imaging Sensors are multi-billion \$ for mobile phone and other cheaper cameras.

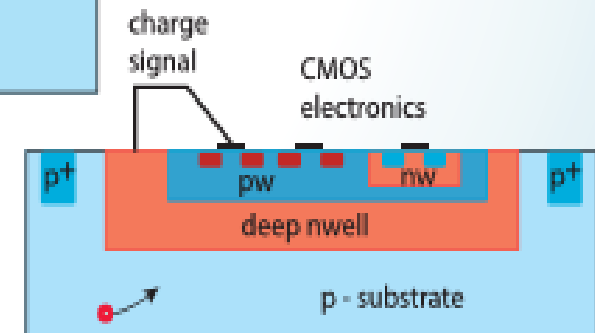
However, applications for space, nuclear, particle and medical physics often need greater radiation tolerance than commercial devices.



Commercial devices have charge collected by **diffusion**



For radiation tolerance collect charge by **drift** with an electric field throughout p - substrate



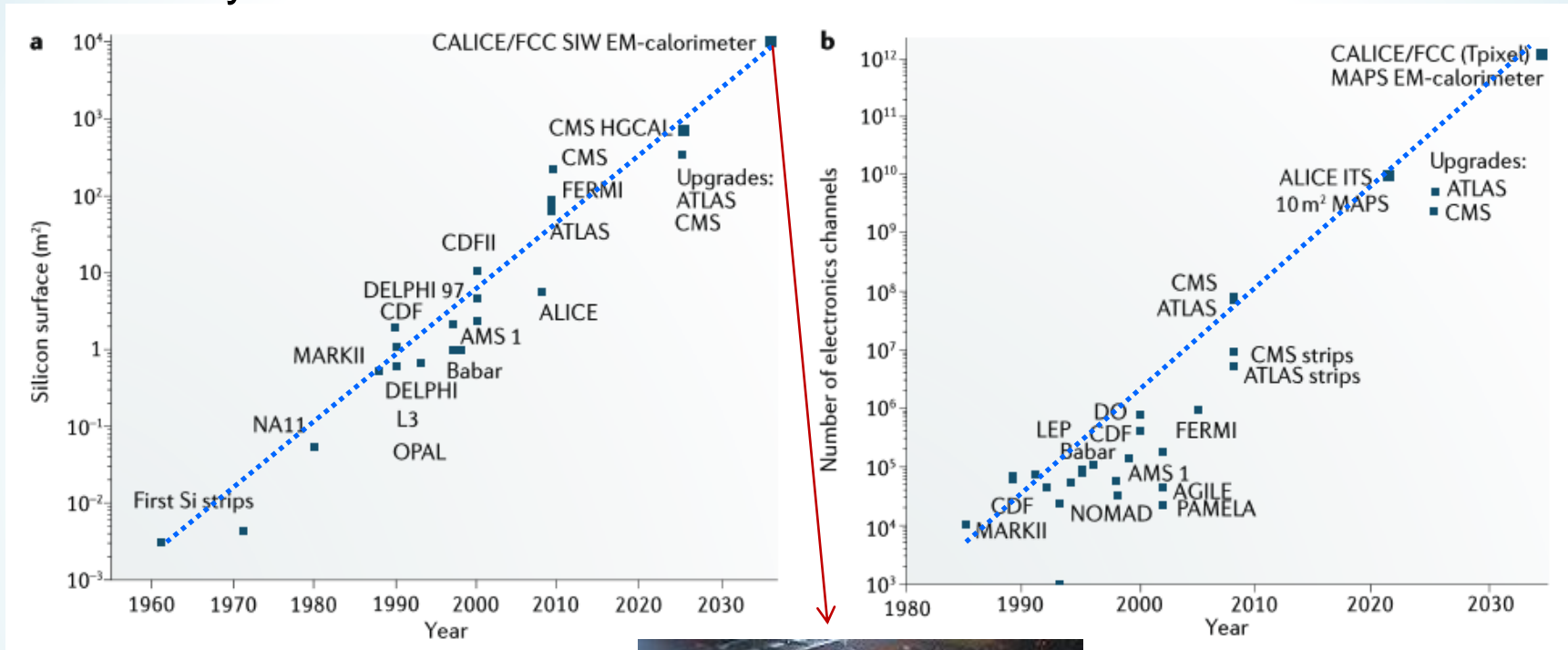
Radiation tolerant  
CMOS **M**onolithic **A**ctive  
**P**ixel **S**ensor (**MAPS**) designs

\*Eva Vilella Figueras (17/5/22)



# Trends Past and Future

More surprising is that some of this exponential behaviour also applies to detector arrays.



# Pulse Mode Ionisation Chamber

(simplest example so instructive to discuss)

Ion chamber contains two parallel electrode plates

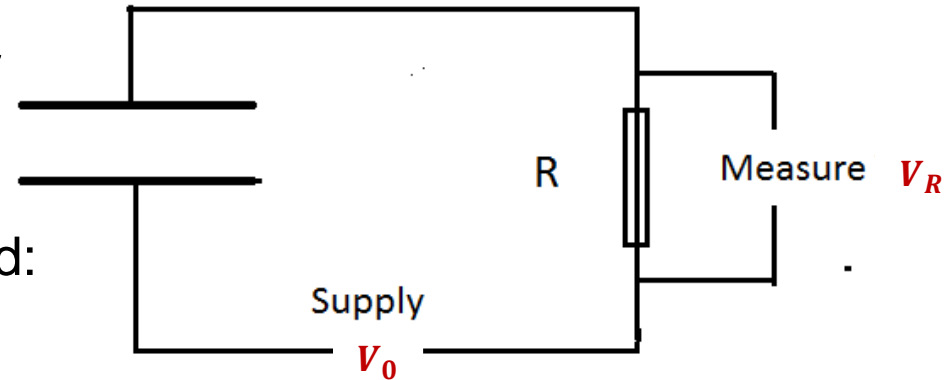
Behaves like a parallel-plate capacitor.

Voltage is supplied via a series resistor

When ion pairs are created in the gas, they start to separate in the electric field:

**ions** move towards **cathode**,

**electrons** towards **anode**.

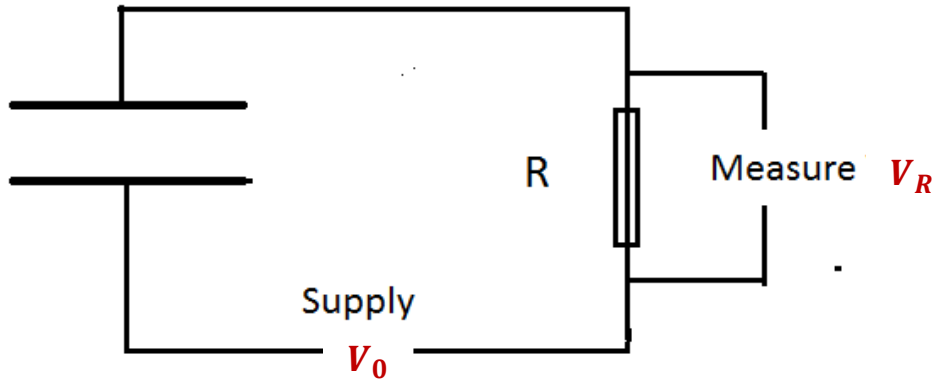


**Separation of charges causes the voltage across the plates to drop**

If this happens much faster than the time constant  $RC$  of the circuit, the voltage drop across the chamber must be balanced by a voltage appearing across the series resistor → **this is the detected signal**.

**Pulse is due to separation of charges, NOT arrival of charges at plates.**

# Pulse Mode Ionisation Chamber



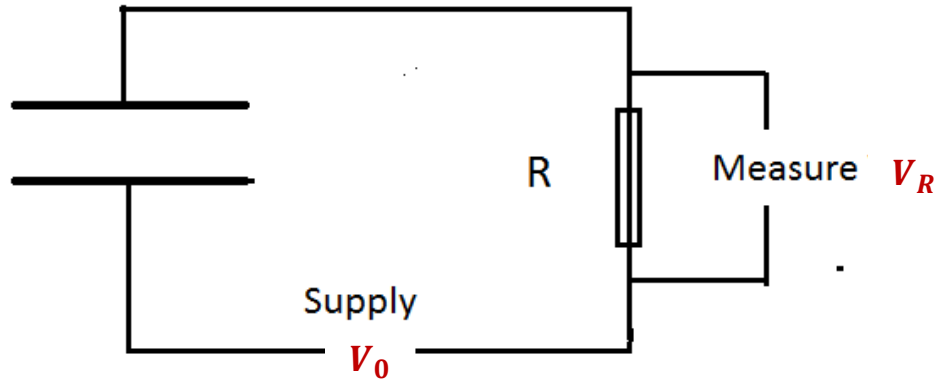
The magnitude  $V_R$  of this voltage drop can be determined from conservation of energy, remembering that the energy stored in a capacitor is given by  $\frac{1}{2}CV^2$ , where  $V$  is the voltage across it.

Initially  $V = V_0$ . Subsequently  $V = V_0 - V_R$

The difference in energy is equal to the work done on the electrons and ions to separate them by the electric field,  $E$ , which is given by  $qEd$ , where  $d$  is the distance moved by charge  $q$ .

$$\text{So } \frac{1}{2}CV_0^2 = \frac{1}{2}C(V_0 - V_R)^2 + qEd_+ + qEd_-$$

# Pulse Mode Ionisation Chamber



Proper treatment that generalises to multiple electrodes uses Ramo-Shockley theorem → [next lecture](#)  
Philipp Windischhofer

$$\text{From } \frac{1}{2} CV_0^2 = \frac{1}{2} C(V_0 - V_R)^2 + qEd_+ + qEd_-$$

$$\text{rearrange to get, } CV_0V_R - \frac{1}{2} CV_R^2 = qE(d_+ + d_-)$$

Since  $V_R \ll V_0$  the second term can be neglected,

$$\text{and so } \boxed{V_R = \frac{qE}{CV_0} (d_+ + d_-) = \frac{q}{cd} (d_+ + d_-)} \quad (\text{since } E = \frac{V_0}{d})$$

When both sets of charges reach the electrodes,  $d_+ + d_- = d$  so  $V_R = \frac{q}{C}$

→ final pulse size is as expected.

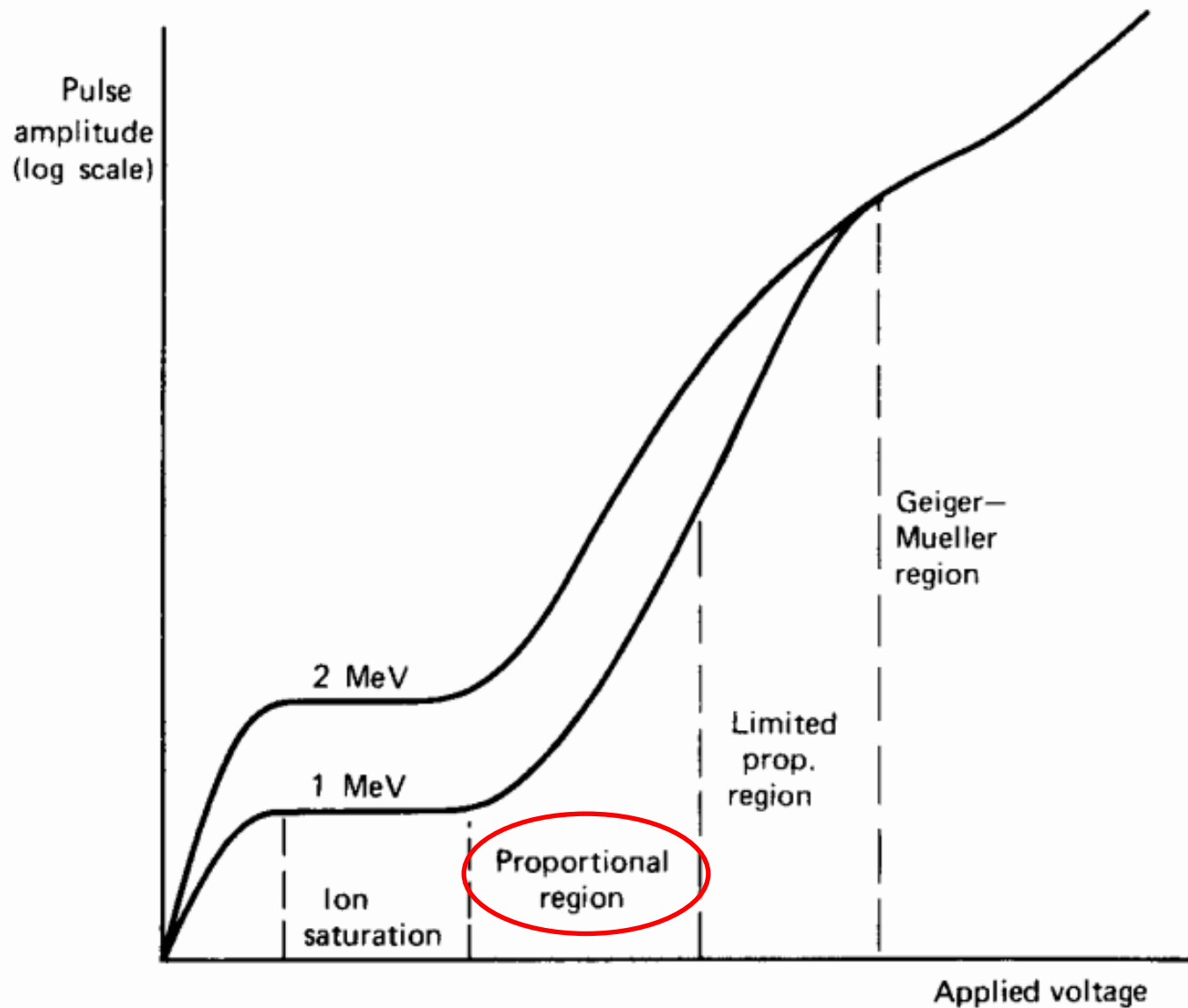


**Figure 6.2** The different regions of operation of gas-filled detectors. The observed pulse amplitude is plotted for events depositing two different amounts of energy within the gas.

# Gas Multiplication

As the electric field increases, electrons gain more energy between collisions with gas molecules.

Eventually (at a field strength of around  $10^6$  V/m) they have sufficient energy to ionise the next molecule they hit.

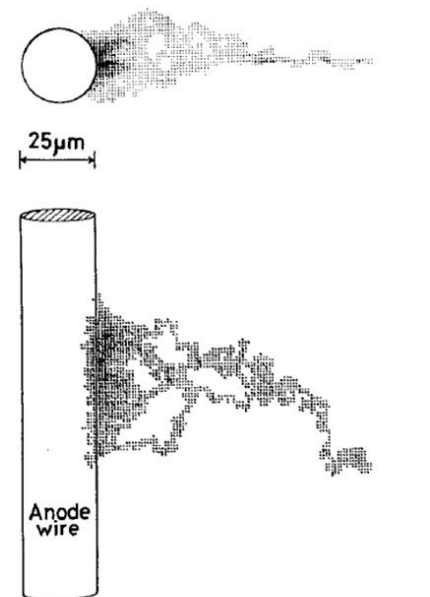
Then each electron/molecule collision releases a further electron, which in turn can ionise further molecules – get a chain reaction, producing an “**avalanche**” of further ionisation.

Total ionisation is much greater than the original ionisation produced by the incident particle – “**gas multiplication**”

Proportional counters typically have cylindrical geometry with central thin anode wire.

Electric field is proportional to  $1/r$ ,

and gas multiplication only occurs in a relatively small volume **close to the anode wire**.



# Gas Multiplication

Note that it is the **electrons** that cause gas multiplication.

Some gases (including oxygen) have a tendency to capture free electrons, forming slow-moving negative ions, which would prevent gas multiplication.

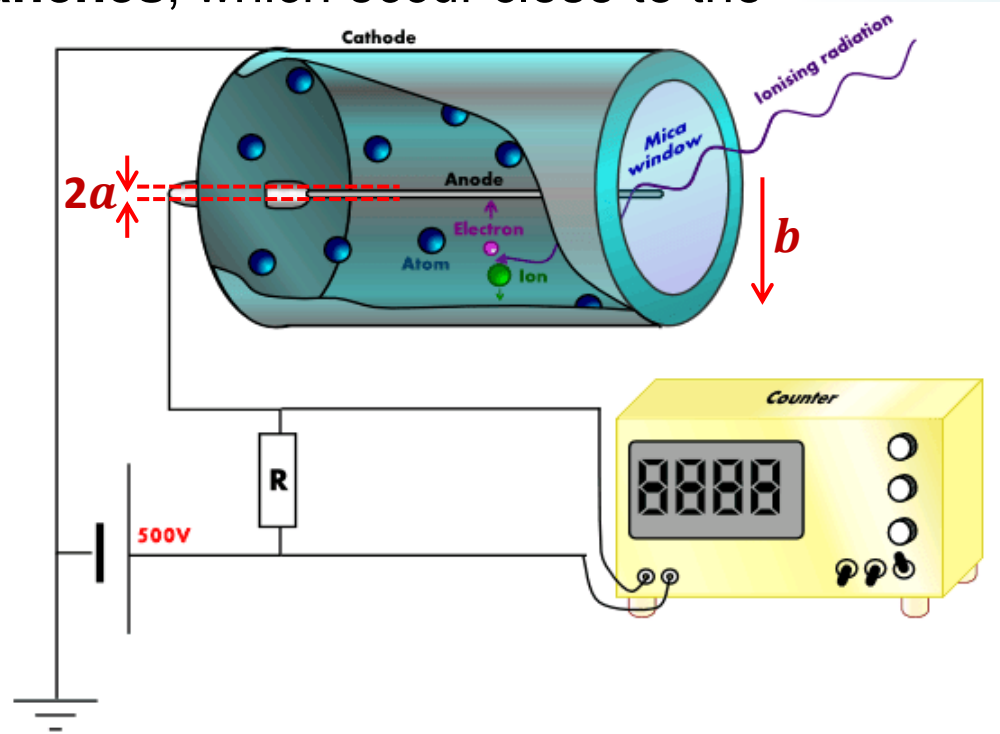
**For proportional counter operation one has to exclude such gases.**

Gas multiplication factor is typically  $10^2$ - $10^4$ . Ionisation in a proportional counter is dominated by the **avalanches**, which occur close to the **anode** wire.

If the radii of the anode wire and the outer cathode are  $a$  and  $b$ ,

since  $E \propto \frac{1}{r}$  and  $\int_a^b E dr = V$ ,

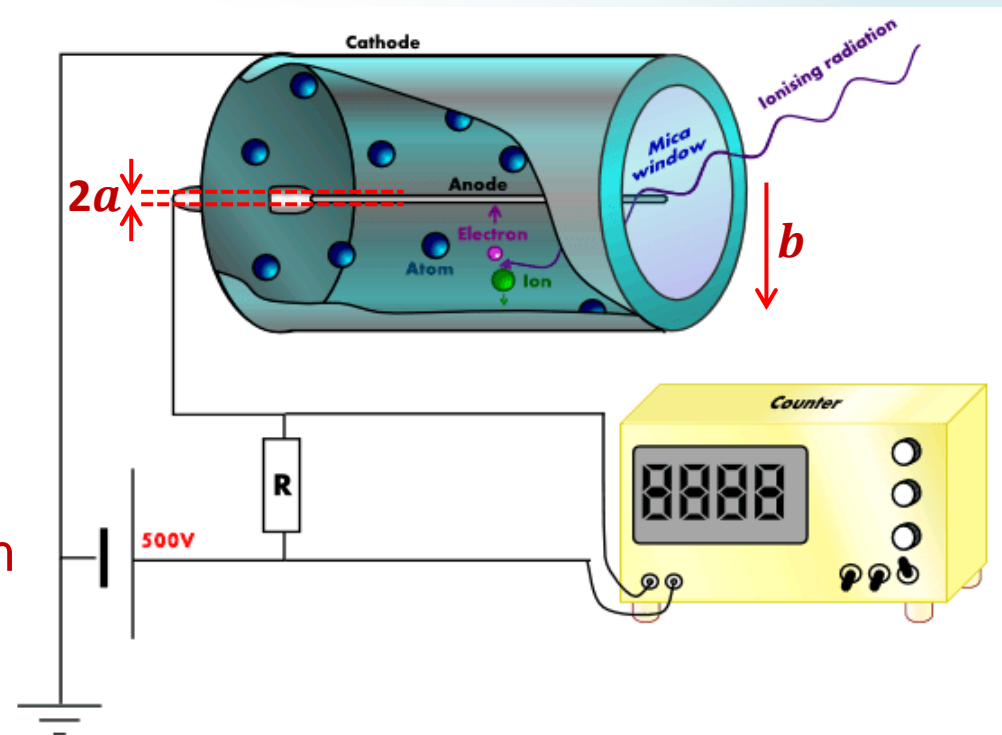
can show that  $E = \frac{V}{r \ln\left(\frac{b}{a}\right)}$



$$E = \frac{V}{r \ln\left(\frac{b}{a}\right)}$$

Typical values  $a = 0.01$  cm (anode wire  $200\mu\text{m}$  diameter),  $b = 1$  cm,  $V = 1000$  V,  $\rightarrow$  field exceeds  $10^6$  V/m when  $r < 0.2$  mm

So avalanches are created very close to the anode wire.



As before, there are two contributions to the pulse (measured as a voltage drop across a series resistor): ions (slow) and electrons (fast).

But **electron** contribution is **very small** since they travel only a **very short distance**.

**Pulse is mainly due to the +ve ions drifting outwards.**

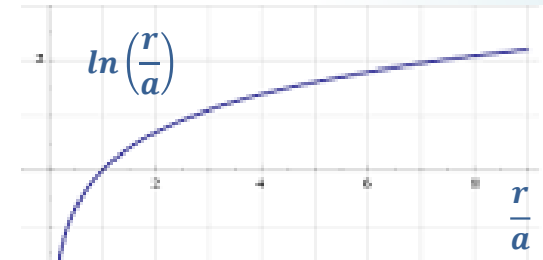
It takes a long time for these to reach the cathode, but fortunately **most of the pulse develops much faster**.

Assuming that the pulse is purely due to **+ve ions** moving outwards from  $r \approx a$ , can, as before, derive the voltage drop  $V_R$  for when the ions have reached a radius  $r$  using the energy relationship:

**energy lost in capacitor = work done on charges.**

So  $\frac{1}{2} CV_0^2 = \frac{1}{2} C(V_0 - V_R)^2 + \int_a^r qE dr$  gives approximately  $V_R = \frac{q}{CV_0} \int_a^r E dr$

$$\rightarrow V_R = \frac{q}{CV_0} \int_a^r \frac{V_0}{r \ln\left(\frac{b}{a}\right)} dr = \frac{q}{C \ln\left(\frac{b}{a}\right)} \ln\left(\frac{r}{a}\right)$$



As expected, as  $r \rightarrow b$ ,  $V_R \rightarrow \frac{q}{C}$

For the time dependence, from the relationship for drift velocity

can use  $\frac{dr}{dt} = v_{\text{Drift}} = \mu E = \frac{\mu V_0}{\ln\left(\frac{b}{a}\right)r}$  and so  $\int_a^r r dr = \frac{\mu V_0}{\ln\left(\frac{b}{a}\right)} \int_0^t dt$

$$\int_a^r r dr = \frac{\mu V_0}{\ln\left(\frac{b}{a}\right)} \int_0^t dt$$

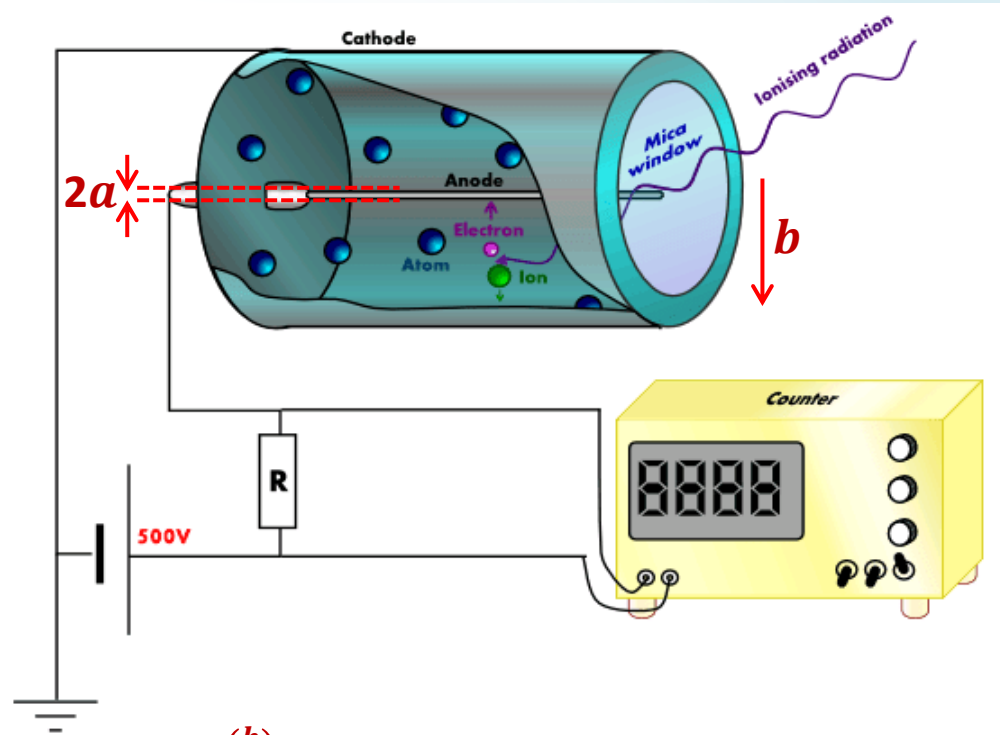
From  $\int_a^r r dr = \frac{1}{2}(r^2 - a^2)$

$$= \frac{\mu V_0}{\ln\left(\frac{b}{a}\right)} \int_0^t dt = \frac{\mu V_0}{\ln\left(\frac{b}{a}\right)} t$$

find the time,  $t$ , to reach radius  $r$  as  $t = \frac{\ln\left(\frac{b}{a}\right)}{2\mu V_0} (r^2 - a^2)$

Taking  $a=0.01\text{cm}$ ,  $b=1\text{cm}$ ,  $V=1000\text{V}$ , and  $\mu=10^{-4}\text{m}^2/\text{Vs}$ ,  
the time to reach the cathode is around **2 ms** (very long!)

But **50%** of the pulse height is achieved when  $\ln\frac{r}{a} = 0.5\ln\frac{b}{a}$  ie  $r=0.1\text{ cm}$ ,  
which happens at a time around **20μs**.



# Semiconductor Detectors

Poisson's equation in **1D** gives:  $\frac{d^2\phi}{dx^2} = -\frac{\rho}{\epsilon}$

Within the depletion layer, assume all dopants ionised, so have charge density  $-eN_A$  on the **p-type** side and  $+eN_D$  on the **n-type** side.

Integrating once, we find the electric field  $E = -\frac{d\phi}{dx}$  **varies linearly**, so  $\frac{dE}{dx} = \frac{\rho}{\epsilon}$ .

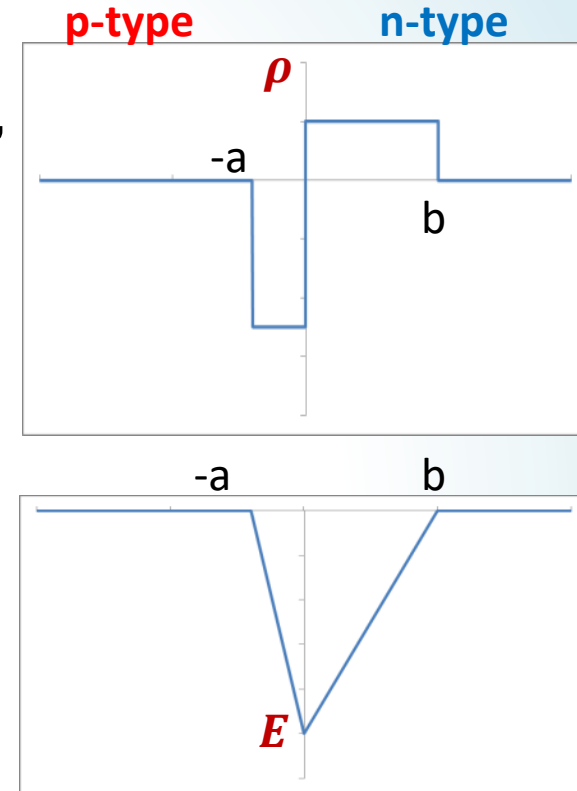
The solution with  $E = 0$  outside the depletion layer is

$$E(x) = -\frac{eN_A}{\epsilon}(x + a) \quad \text{for } -a < x < 0,$$

$$E(x) = \frac{eN_D}{\epsilon}(x - b) \quad \text{for } 0 < x < b.$$

Since  $E$  must be continuous at  $x = 0$  we require  $aN_D = bN_A$  (conserves charge): layer goes deeper on side with lower doping.

Signal depends on  $qE(x)d$  so contributions of electrons and holes are different and more complicated, but total integrated signal is still given by the charge deposited.

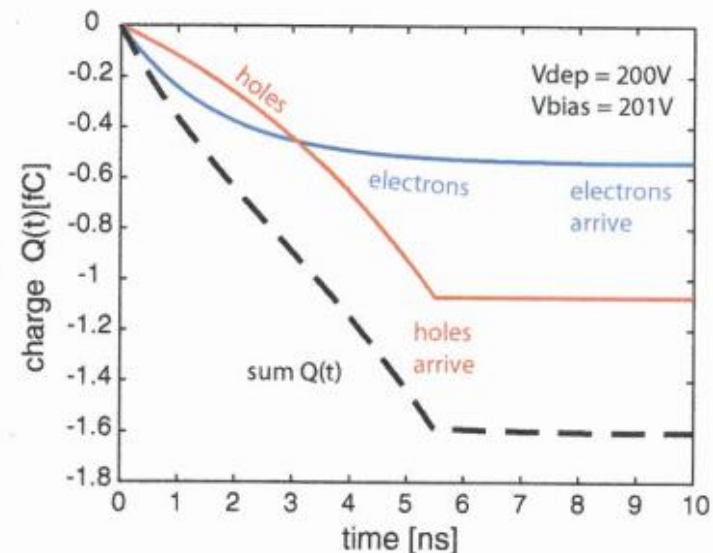
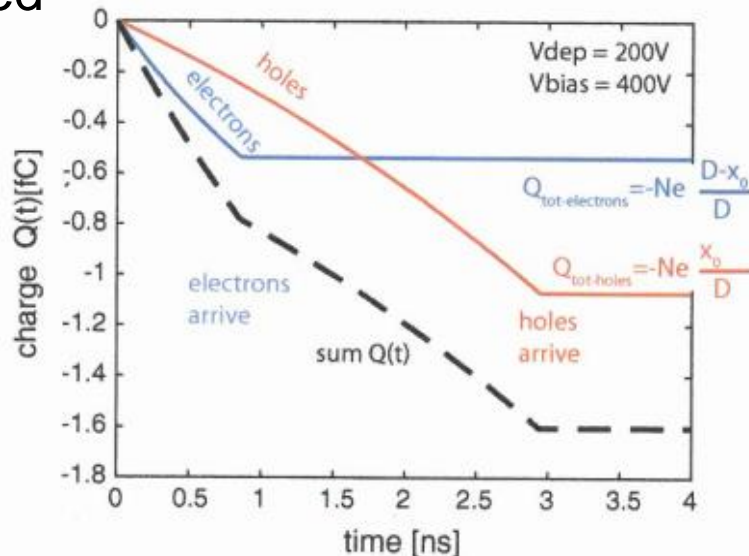
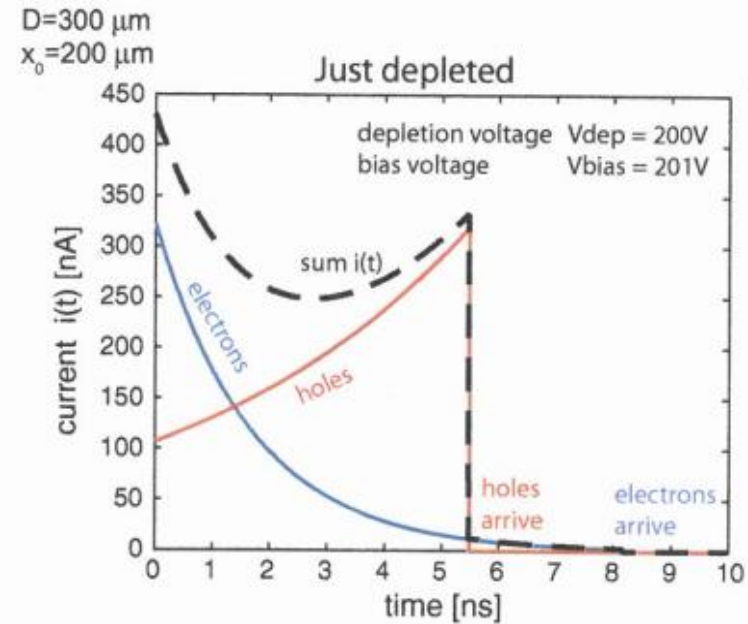
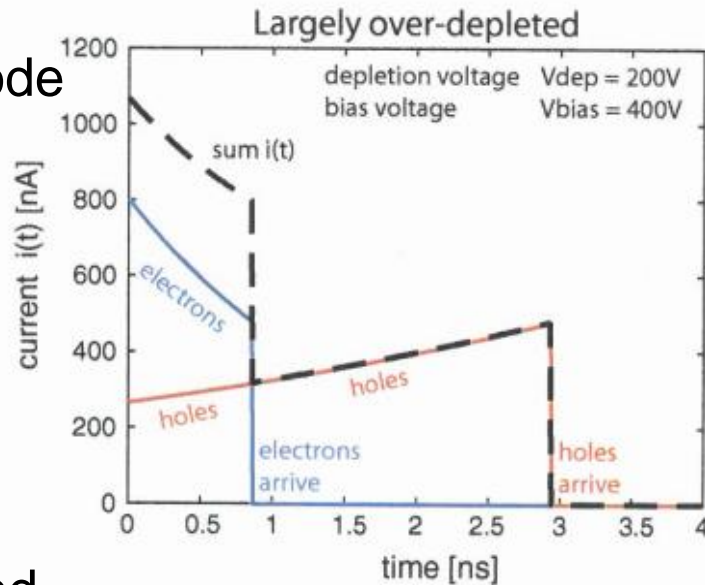


# Semiconductor Detectors

$p^+$  implanted  
 $n^-$  substrate diode

(Very simple  
1D example)\*

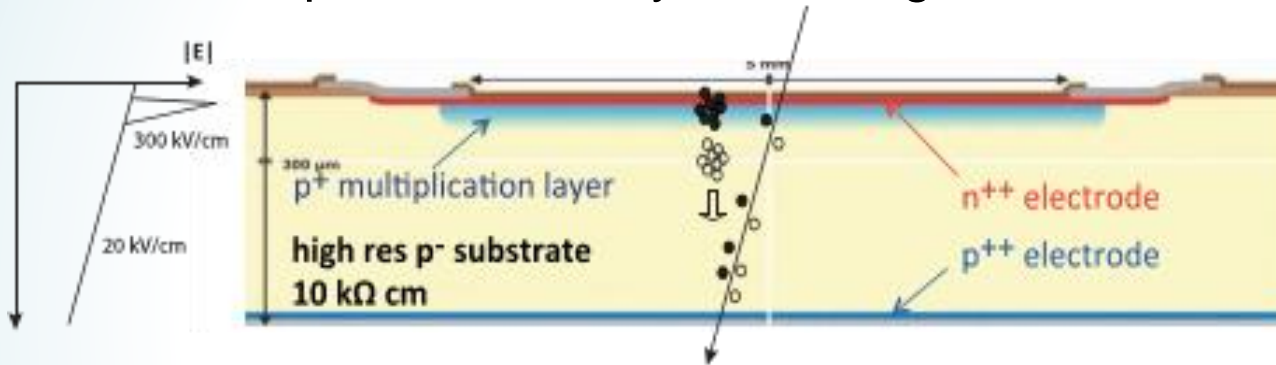
10000 eh pairs  
(1.6 fC) deposited  
at  $x_0 = 200\mu\text{m}$   
below the  
 $p^+$  electrode in  
a  $300\mu\text{m}$  thick  
silicon diode



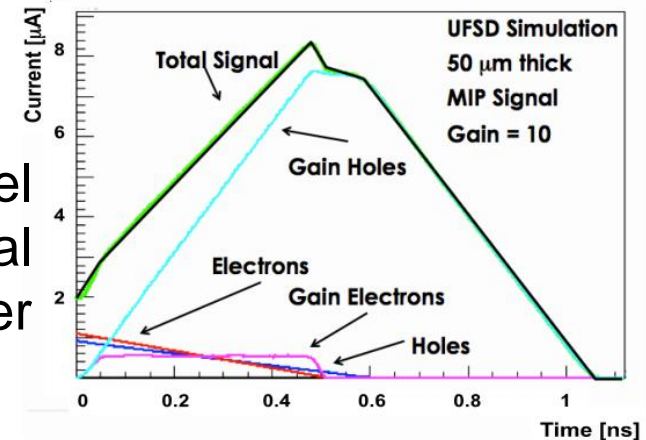
\* For segmented case see  
[next lecture](#) by Philipp Windischhofer

# Fast Timing Detectors

Silicon detectors can be designed to give fast signals\* operating in a mode where the field is high enough (**several  $\times 10^5 \text{V/cm}$** ) for the drifting charge to accelerate to high enough energy between collisions to create further electron-hole pairs when they do undergo collisions.



Fast timing pixel  
with built-in signal  
multiplication layer



\*Francisca Munoz Sanchez (10/5/22)

# Gas Proportional Counter Energy Resolution

The size of the final signal is proportional to the product of the initial charge released and the gas multiplication factor:  $V \propto NM$ , where  $N$  is the **number of avalanches** and  $M$  is the **average multiplication factor**. Both these quantities are subject to independent statistical fluctuations which contribute to the energy resolution in quadrature.

As before,  $N = \frac{E}{w}$  and  $\Delta N = \sqrt{FN}$  (where  $F$  is the **Fano factor**) and given that, experimentally, the fluctuations in the multiplication factor are found to be approximately given by  $\left(\frac{\Delta M}{M}\right)^2 \approx \frac{b}{N}$  where  $b \approx 0.5$  (see Knoll).

**Energy resolution** then goes from:  $2.35 \sqrt{\frac{F}{N}}$  to  $2.35 \sqrt{\frac{F+b}{N}} = 2.35 \sqrt{\frac{w(F+b)}{E}}$

As an example, if an X-ray deposits **50 keV**, in a gas with  $w=30$  eV,  $F=0.1$  and  $b=0.5$  this predicts FWHM energy resolution of approximately **4.5%**.